Science of the Total Environment 1004 (2025) 180787

Contents lists available at ScienceDirect

Science of the Total Environment

journal homepage: www.elsevier.com/locate/scitotenv

Combining porewater profiles and batch tests to quantify redox reactions and heavy-metal(loid)s release potentially induced by managed aquifer recharge

Nicolò Colombani [a,*], Abraham Ofori [b], Jonathan Domizi [a], Matteo Gisolo [c], Silene Itala Cresseri [c], Micòl Mastrocicco [b]

[a] SIMAU – Department of Materials, Environmental Sciences and Urban Planning, Polytechnic University of Marche, Via Brecce Bianche 12, 60131, Ancona, Italy
[b] DiSTABiF – Department of Environmental, Biological and Pharmaceutical Sciences and Technologies, Campania University "Luigi Vanvitelli", Via Vivaldi 43, 81100, Caserta, Italy
[c] A2A Ciclo Idrico S.P.A., Via Alessandro Lamarmora 230, 25124, Brescia, Italy

HIGHLIGHTS

- To evaluate MAR suitability in urban area 2 cores were drilled.
- High permeability layers are present and good recharge rates can be achieved.
- Kinetic batch experiments at different depths ensured good groundwater quality.
- Sequential extractions quantified low mobility of heavy metal(oids) by recharge water.

GRAPHICAL ABSTRACT

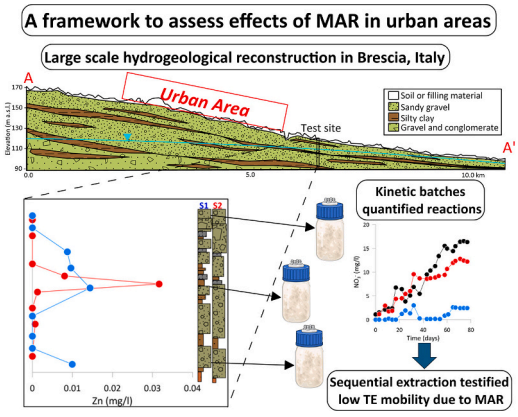

ARTICLE INFO

Keywords:
Porewater quality
Vadose zone
Trace elements
Sequential extraction
Groundwater replenishment

ABSTRACT

Like other highly populated alluvial plains, the Po plain (Italy) is suffering from groundwater reserves' decline and widespread pollution since the last two decades. Managed aquifer recharge (MAR) is often used for aquifer replenishment and to mitigate groundwater contamination. Brescia, located in the middle of the Po plain, with its 200 k inhabitants and a wide industrial area exerts large pressures on the groundwater quality and could benefit of MAR. To evaluate the interactions among MAR water and aquifer matrix, two cores were drilled in an urban/industrial area to capture the lithological variability of the unconfined aquifer and to delineate redox gradients. To this purpose, vertical profiles of soil cores were collected via Rhizon samplers and analysed for grain size, TDS, pH, Eh, DOC, major ions, and trace elements. In addition, 3 batches with 160 g of sediment and 800 mL of deionized water were set-up in an inert atmosphere (N_2) and monitored for 3 months. Stratigraphical cores

* Corresponding author.
E-mail address: n.colombani@univpm.it (N. Colombani).

https://doi.org/10.1016/j.scitotenv.2025.180787
Received 6 May 2025; Received in revised form 3 October 2025; Accepted 21 October 2025

results were used to locate the most permeable layers to maximize MAR injection efficiency. The porewater composition of depth profiles revealed that possible pollution sources could be untreated wastewaters from leaking sewers or overflows rather than industrial contamination. The batches and sequential extraction demonstrated that no significant release of heavy-metal(loid)s was induced by MAR water and the already present contaminants were diluted below admissible limits. Pre- and post-experimental characterization of Fe-mineral phases via sequential extraction, suggested a >50 % ± 25 increase of crystalline Fe-oxides at shallow depths that can further decrease heavy-metal(loid)s mobility. The proposed framework could be employed in other environments to assess the feasibility of MAR prior to perform a full-scale trial and to assist tailored design solutions.

1. Introduction

The Po plain and its aquifers are under stressed conditions by intense anthropogenic activities like: widespread urbanization (Vittori Antisari et al., 2010), agriculture (Lasagna et al., 2016; Martinelli et al., 2018; Pinardi et al., 2022), and industrial facilities (Tiwari et al., 2017), as many other alluvial aquifers around the world. Given the water scarcity of recent years and that medium and long-term forecasts do not contemplate significant water surpluses in the Po plain (Musolino et al., 2018), but rather an extremization of weather and climate phenomena, this will necessarily increase surface runoff and decrease effective infiltration (Montanari, 2012). The decreased groundwater recharge is already threatening the groundwater dependent ecosystem of the "Fontanili" (Balestrini et al., 2021), which are semi-natural lowland springs located along the transition zone between the high and low in the Po plain (Giuliano, 1995). This springs' belt is also known to be affected by widespread nitrate contamination (Sacchi et al., 2013), that will be exacerbated by the intensification of summer droughts due to climate changes (Rotiroti et al., 2023). To contrast the groundwater resources depletion and groundwater quality deterioration, an adaptation strategy might be the implementation of managed aquifer recharge (MAR) techniques (Dillon et al., 2019).

MAR could be implemented using different techniques, like infiltration ponds and basins (Pokhrel et al., 2023; Racz et al., 2012), recharge wells and infiltration trenches, gravity driven or with pump injection (Martinez et al., 2022). Agricultural MAR can be set up through a variety of irrigation techniques (Levintal et al., 2022) but must avoid agrochemicals leaching, like pesticides residues (Zhou et al., 2024) and nutrients (Levintal et al., 2023) that are often persistent in the environment. Other possible drawbacks of MAR are the unwanted introduction of mobile and persistent contaminants of emerging concern, like PFAS or personal care products (Mumberg et al., 2024). Finally, oxic waters used in MAR often provoke large changes in reducing environments, like the release of potentially toxic trace elements (Riedel et al., 2022) via amorphous and crystalline phases dissolution or surface complexation reactions (Vergara-Sáez et al., 2024). While field-based studies can capture the overall redox status or redox environments shifts, laboratory-based studies allow to unravel biogeochemical processes more in detail despite the simplified conditions of constant temperature, pressure, and solutes exchange (Zhang & Furman, 2021). In this study, both field observations and laboratory experiments were employed to envisage the possibility of infiltrating high purity water (here deionized water), often used as proxy of reclaimed water from quaternary wastewater treatment plants (Schafer et al., 2021). The MAR scheme using vertical injection wells, could help to contrast the unconfined aquifer depletion that already affected this area over the last two decades and could help to dilute the presence of anthropogenic contaminants (Pili et al., 2017). To assess whether the proposed MAR could promote biogeochemical reactions that may alter the groundwater quality (Guo et al., 2023), it is necessary to characterize the solid matrix of the aquifer and its vertical variability (presence of fine-grained lenses) near the recharge point, the major inorganic contaminants of geogenic origin in the Po plain sediments (Zanchi et al., 2022; Schiavo et al., 2024), and the eventual presence of contamination of anthropogenic origin (Zanotti et al., 2022).

The evaluation of the presence of heavy metals and metalloids within the solid matrix of the aquifer and their effective mobility was estimated using the sequential extraction technique proposed by Sun et al. (2016) and modified by Sbarbati et al. (2020). The target inorganic contaminants were Al, As, Cd, Cr, Fe, Mn, Ni, Pb, V, and Zn. Among these, As is by far the most reactive and the one that can potentially be brought into solution by aquifer recharge interventions (Fakhreddine et al., 2021). The stable forms of As dissolved in natural waters are mostly oxyanions of As(V) and As(III), respectively in oxidizing and reducing conditions (Sadiq, 1990). pH and redox conditions are the two factors that most influence the geochemistry of As in the environment and therefore its mobility. In general, As(III), more toxic than As(V), is more mobile since it is absorbed in smaller quantities (Colombani et al., 2015; Pena et al., 2005). Studies conducted on the As absorption mechanisms indicate that the dissolved concentrations of As(V) and As(III) vary mainly as a function of the quantity of Fe-oxides, Al-oxides, and clays present in the solid matrix (Suda and Makino, 2016). Since MAR techniques are evolving fast with the improvements in water treatment technologies, site specific planning is required to holistically consider future water availability and quality to anticipate potential geochemical interactions and protect groundwater quality (Fakhreddine et al., 2021). To date, laboratory experiments like batch and column experiments have been conducted in tailored MAR solutions to evaluate the potential removal of organic (Maeng et al., 2011; Regnery et al., 2016) and inorganic pollutants like bromate (Wang et al., 2018), to quantify As mobility triggered by high purity water injection (Fakhreddine et al., 2015), or to delineate major ions geochemical changes (Ronen-Eliraz et al., 2017); but so far kinetic batch experiments that concomitantly evaluate the major and trace elements geochemistry are still rare.

This paper aims to present a novel framework to characterize the possible hydrogeochemical impacts of high purity waters employed by MAR in alluvial aquifers, with special reference to redox sensitive species and heavy-metal(loids)s, like As. The major novelty of this work consists in the combination of field-based data (stratigraphic and hydrogeological information coupled with undisturbed porewater profiles) with laboratory-based data (kinetic batch experiments and sequential extraction) to gain a comprehensive understanding of the possible interactions among injected high purity oxic waters and aquifer matrix induced by MAR, to screen and forecast possible pitfalls prior to implement a full scale trial.

2. Materials and methods

The framework consists of 5 stages: (i) literature study on hydrogeological settings to locate the drilling site, (ii) drilling at test boreholes to collect sediment samples and preserve them in an inert environment, (iii) porewater profiles extraction and analysis to reconstruct the main redox zones and reactions, (iv) kinetic batch tests with infiltrating water to quantify eventual metal release and other relevant reactions, and (v) pre and post batches sequential extraction to elucidate possible shift in reactive mineral phases, such as Fe-oxides. In the following sections each stage will be further explained and examined using the Brescia suburban area as a case study representative of the upper Po plain

stratigraphical architecture.

2.1. Study area hydrogeological setting

The upper Po plain is filled with Plio-Quaternary sediments with a gradual thinning northward (Castaldini et al., 2019). The sedimentary infill exhibits a shallowing upward trend, transitioning from deep-marine Pliocene deposits to shallow-marine and continental Quaternary deposits (Ori, 1993). The region is characterized by extensive alluvial fans, composed of Late Pleistocene fluvioglacial deposits, and a cyclic change in fluvial-channel stacking pattern, reflecting glacial-interglacial periods during the Middle-Late Pleistocene.

The flat areas of Brescia are characterized by alluvial and fluvioglacial deposits for a thickness that can locally exceed 250 m. The area owes its genesis to the intense depositional activity carried out by the Mella river during the Quaternary and to the significant erosive phenomena that affected the mountainous reliefs behind it (Fig. 1).

In the pre-Quaternary era, the Mella river flowed inside a deep valley, then filled by Villafranchian deposits consisting of grey and grey-blue clays and silty clays constituting the bottom aquiclude. Above this confining layer, two hydrogeological units can be distinguished: i) a conglomeratic unit formed by ancient alluvial deposits that can be related to the ferralitic deposits of the Middle Pleistocene (Marchetti et al., 2001), with a thickness ranging from 30 to 200 m that progressively decreases from N to S and moving away from the axis of the Mella river. This unit hosts the first confined aquifer, sometimes locally semiconfined; ii) a sandy gravel unit represented by coarse gravelly-sandy lithologies corresponding to alluvial deposits of the Upper Pleistocene and Holocene with a thickness of 30–50 m. This unit hosts the unconfined aquifer that shows a groundwater flow direction towards South, influenced by surface water interactions and groundwater pumping (Zanotti et al., 2023). The boundaries between the two units are not well defined since there are neither morphological, nor lithological or pedological elements allowing a clear distinction. The lateral boundaries occur mainly with erosive surfaces, while the vertical ones show the superposition of both positive and negative depositional sequences.

At the top of the sequence, soils are deep to moderately deep, with common skeleton on the surface and frequent in depth, with medium to fine texture, neutral to alkaline pH and good drainage. The permeability of the vadose zone is high (Zanotti et al., 2022) thus allowing rainfall infiltration except for the paved urban environment. The permeability map of the unconfined aquifer retrieved from the Lombardy Region Technical Map web portal (https://www.geoportale.regione.lombardia.it/) also indicates an elevated permeability of the sandy gravel unit. The mean hydraulic conductivity value, retrieved from the analysis of 6 pumping tests in wells located near the tests site (ISPRA national boreholes database, 2024) and tapping the sandy gravel unit, was $3.1*10^{-4}$ m/s with a standard deviation of $3.8*10^{-4}$ m/s; indicating a good permeability of the unconfined aquifer, but also a high degree of heterogeneity. Much less information is available on the permeability of the conglomeratic unit, although it is considered a productive unit when the degree of cementations is poor (Bonomi et al., 2014). The mean hydraulic conductivity value retrieved from the analysis of 4 wells tapping the conglomeratic unit (ISPRA national boreholes database, 2024) was $6.4*10^{-5}$ m/s with a standard deviation of $7.0*10^{-5}$ m/s. This indicates a moderate permeability of the confined aquifer and again a high degree of heterogeneity. Thus, the test site has good potential for MAR given the high capacity of the aquifer system to infiltrate water.

2.2. Climatic data and hydrological water budget

The climate retrieved from Copernicus Interactive Climate Atlas using the ERA5-Land Climatology - Historical - 1961-1990 - Annual dataset (https://atlas.climate.copernicus.eu/atlas) is moderately

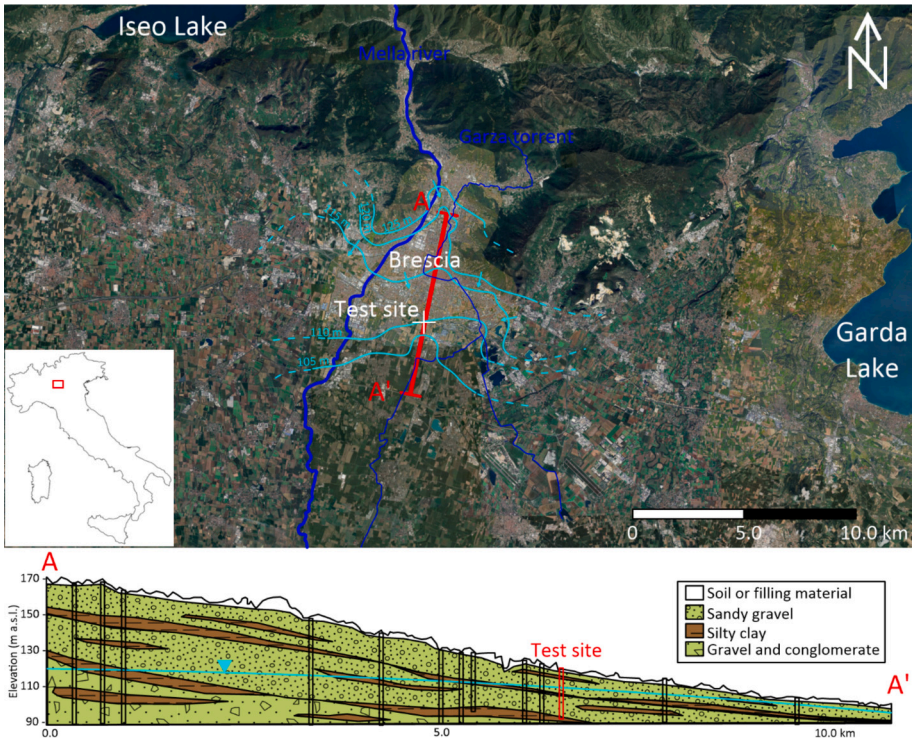

Fig. 1. Upper panel: Landsat image of the study area in December 2020 (source Google Earth) with the location of the test site (white cross), the piezometric map in m a.s.l. (cyan lines), the main and secondary rivers (blue lines), and the hydrogeological cross section (red line); lower panel: 2D sketch of the hydrogeological units and the water table (cyan line), the vertical exaggeration is 1:125.
The piezometric map was redrawn from the Brescia Municipality Environmental Report (2022), while the 2D sketch was drawn using the ISPRA (2024) national boreholes database.

continental, with a mean annual total precipitation of 1143 mm. The latter has slightly decreased (towards 1113 mm/y) in the last 3 decades (change from 1995–2014 to 1991–2020). The historical (1961–1990) mean annual temperature is 10.24 °C and had a positive decadal anomaly of +0.47 °C in the last 3 decades (change from 1995 to 2014 to 1991–2020), while the mean annual evaporation passed from 624 mm/y in the 1961–1990 period to 675 mm/y in the 1991–2020 period.

These climatic anomalies, produced an exponential increase of the soil water deficit in the Lombardy region and an exponential decrease of groundwater recharge (Fig. 2) as calculated via the Nationwide GIS-based regular gridded hydrological water budget procedure BigBang 8.0 (https://www.isprambiente.gov.it/pre_meteo/idro/BIGBANG_ISPRA.html) for the 1951–2023 period. Detailed information on the procedure employed to compute the water balance can be found in Braca et al. (2022).

Both climatic data and the hydrological water budget highlight the urgent need for MAR implementation to augment the groundwater resources in this area.

2.3. Core logs drilling at the test site

To assess the effective capability to inject excess water near the facilities of the A2A multiutility company located in Brescia were selected as a source of infiltration water for MAR operation. Here, two cores were drilled 100 m apart, named S1 and S2 down to a depth of 32 m below ground level (b.g.l.). A continuous coring technique without the use of detergents or lubricants was employed, and the core barrels were cleaned with deionized water at the end of each log to avoid external contamination and "cross-contamination". Subsequently, the boreholes were screened in the main aquifer from 10 to 30 m b.g.l. to be potentially employed as vertical infiltration wells with a nominal injection rate of 1.0 l/s each, this would ensure a relatively small groundwater mounding around the wells to avoid any possible back surge. A total of 30 sediment samples per core log were retrieved, approximately one per meter. The sediments samples were divided into aliquots of 4–5 kg and immediately placed in vacuum bags to minimize the contact with the oxidizing atmosphere, transported to the laboratory the same day of collection and stored at 4 °C.

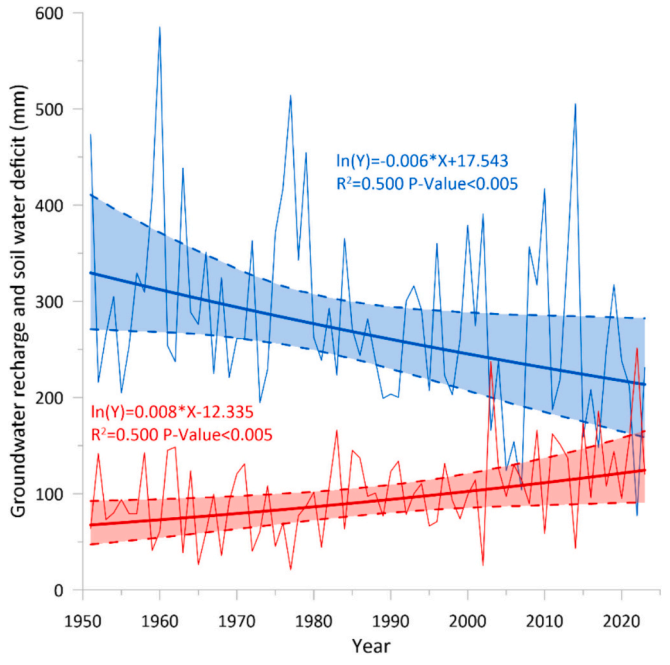

Fig. 2. Trends for the period 1951–2023 for the Lombardy region of calculated yearly groundwater recharge rate (thin blue line) and soil water deficit rate (thin red line). Fitted exponential laws (thick lines and formulas) and their 95 % confidence intervals (shaded areas within dashed lines) are also depicted.

2.4. Analytical methods

Once in the lab, the sediment samples were inserted into a Glove-Bag (Cole-Parmer, USA) filled with ultrapure nitrogen gas (Airliquid N_2, Italy) and the porewater was sampled using Rhizon MOM samplers (Rhizosphere Research Products, The Netherlands). Rhizon MOM samplers, which have a glass fibre wire as strengthener, are suitable for the extraction of fluids from unsaturated porous media for environmental purposes. Rhizon MOM samplers were used instead of sampling groundwater in a post drilling stage via multi-level samplers, since they collected directly the groundwater present within each single core sample, thus providing unbiased high resolution chemical gradients of the dissolved species present in each log. The samples, from which an aliquot of at least 10 mL was retrieved, were 9 for S1 and 9 for S2. Then the sediments particle-size distribution was determined by dry sieving and the pipette method (Miller and Miller, 1987) for all the collected samples.

Three sediment samples were selected (S1–10, S1–20, and S1–29.5) to represent the vertical physical-chemical heterogeneities recorded on site, and were also considered as replicates of the saturated portion of the unconfined aquifer. In fact, this would be the vertical section interested by the MAR injection, thus their analyses could deepen the understanding on the leachable fraction. To quantify the possible reactions between the injected deionized water (18 MΩ) and the aquifer matrix, batches were set up in 1000 mL glass containers with 160 g of equivalent dry sediment and 800 mL of oxic deionized water (see Supplementary materials for composition). The containers were sealed with a headspace cap and Viton rubber for the sampling of 2 aliquots per week for a period of 3 months. The batches were incubated in the dark at constant temperature. TDS, pH, ORP, dissolved O_2, and temperature were measured using a portable multiparameter probe Hi9829 (Hanna Instruments™). Extracts from the samples were filtered through a 0.45 μm membrane filter (MF-Millipore, USA), stored in low density polyethylene vials (10 mL), and kept in a refrigerator until further analysis.

Porewater concentration C_{pw} was derived according to Appelo and Postma (2005):

$$C_{pw} = C_w * \frac{V_w * \rho_b}{S} \frac{}{n} \quad (1)$$

where V_w is the volume of water used (mL) in the batches, C_w (mg/L) is the concentration of the analysed dissolved species, S is the sediment dry weight (g), ρ_b is the dry bulk density (g/cm^3) and n is the sediment porosity (mL/mL).

The major anions (including F^-, Cl^-, Br^-, NO_3^-, NO_2^-, PO_4^{3-}, SO_4^{2-}) were determined by isocratic ion chromatography (DIONEX, ICS-1000) equipped with an AS-14 column and a guard column, an electrolytic suppressor ASRS-500 and an AS-40 autosampler. The detection limit for each ion was 10 μg/L, and the analyses were within a relative standard deviation of ±3 % over three replicas per sample. Cations (Na^+, K^+, Mg^{2+}, Ca^{2+}) and trace elements (Al, Li, Sr, As, Cd, Cu, Mn, Ni, Be, Cr, Fe, Pb, Se, Si, V, Zn) were determined by inductively coupled plasma–optical emission spectroscopy (ICP-OES, 8300) using a combination of Ar and N_2 as carrier gases. A hydride generation sample introduction system was employed to lower As and Se detection limits. The detection limit for major ions was 10 μg/L and for trace elements was 1.0 μg/L, while the relative standard deviation for cations was ±5 % and for trace elements ±4 %, over three replicas per sample. DOC was analysed with a Pharmacia Biotech Ultrospec 2000 UV/VIS spectrophotometer following the procedure of Cook et al. (2017), with a detection limit of 100 μg/L. Alkalinity was determine titrimetrically, with a detection limit of 100 μg/L.

2.5. Sequential extraction from sediments

Three replicates for each sample employed for the batches (S1-10, S1-20, and S1-29.5) were collected before starting the batch experiments and at day 80 (at the end of incubations) to perform the sequential extraction. The sediment aliquots were subsequently re-divided in an inert environment into sub-aliquots using a hacksaw, and the sediments that have come into contact with the hacksaw were removed with a Teflon spatula. Each sub-aliquot was placed in a 50 mL polycarbonate centrifuge vial. Sequential extractions of As adsorbed on sediments were performed on core samples using published methods (Keon et al., 2001; Sun et al., 2016; Sbarbati et al., 2020), in the sequence highlighted in Table 1. Individual aliquots of sediment (4 g dry weight) were treated sequentially with each extracting solution (solid:solution = 0.01 by mass), the suspensions centrifuged (25 min at 8500 rpm), and the supernatant decanted and filtered (0.45 μm nylon membrane filters). Between each extraction step, the sediments were washed with 40 mL of deionized water (18.2 MΩ), centrifuged, and the supernatant decanted. One-way analysis of variance test (ANOVA) was performed in Microsoft Excel 365 to investigate interrelationships between parameters. ANOVA was employed to examine if there were statistically significant differences in the extraction steps. Statistical significance was specified by a threshold of $*P \leq 0.05$. Analyses of variance were performed on untransformed data and mean separation was accomplished using Tukey's HSD test.

3. Results and discussion

3.1. Detailed stratigraphic logs

The stratigraphy of the S1 log fits very well into the Brescia hydrogeological context (Bonomi et al., 2014), with the unconfined aquifer characterized by a high permeability, as it is formed by unconsolidated gravelly and pebbly debris in a sandy silty matrix. At the bottom of both the log S1 and S2 a compact clay layer was identified as the basal aquitard of the unconfined aquifer, since the other 6 wells with stratigraphy near the test site (ISPRA, 2024) displayed at the same depth a layer from 2.5 to 6.0 m of compact reddish clay.

As can be appreciated from Fig. 3, the vertical variability is elevated, with the presence of low permeability horizons, which possibly limit the vertical mixing of groundwater at a local scale, but contemporary increasing the recharge volume (Wu et al., 2021). These horizons are also much more reactive than gravelly layers as they are characterized by larger specific surface area and therefore by a greater capacity to adsorb and desorb any contaminant of anthropogenic or geogenic origin. For example, they could release As via arsenate desorption from Fe-(hydr)oxides in oxic environments or via oxidative dissolution of As-bearing pyrite from reducing environments (Fakhreddine et al., 2020).

The grain size results show that S1 log has a greater vertical variability compared to S2 log, confirming the notable facies heteropy present in the Holocene hydrogeological unit composing the unconfined aquifer. As shown in Fig. 3, fairly homogeneous sandy gravels layers are interbedded with silty-clay and silty-sand lenses in heterotopic ratio. These lenses have horizontal and vertically variable extensions and are characterized by "flute beak" pinch out (Pili et al., 2017). Overall, the sandy gravel layers encountered in the S1 and S2 logs are on average very permeable and would allow the injection of significant volumes of water, besides the absence of underground infrastructures and the relatively thick vadose zone, makes this area located at the outskirts of the urban environment and in proximity of the A2A facilities a good place to infiltrate large quantities of water. Although, to accurately quantify the possible reactions triggered by the injection of deionized water and the aquifer matrix, additional experiments are needed, as reported in the following sections.

Table 1
As sequential extraction procedure modified from Sbarbati et al. (2020).

Step	Extractant and time	Target Fe phase	Target As phase
1	1 mol/L $MgCl_2$, pH 7, 2 h, one repetition	Exchangeable Fe	Loosely bound As
2	1 mol/L CH_3COONa adjusted to pH 4.5 with CH_3COOH, 24 h, one repetition	Fe carbonates (siderite)	As associated with carbonates, weakly bound As
3	1 mol/L $NH_2OH{\cdot}HCl$ in 25 % v/v CH_3COOH, 48 h, one repetition	Amorphous Fe(III) oxides (ferrihydrite)	As associated with amorphous Fe oxides
4	50 g/L $Na_2S_2O_4$, pH 4.8 with CH_3COOH/ $C_6H_5Na_3O_7{\cdot}2H_2O$, 2 h, one repetition	Crystalline Fe(III) oxides (goethite and hematite)	As associated with crystalline Fe oxides
5	1 mol/L Na_3PO_4, pH 5, 16 h & 24 h, one repetition for each period	–	As adsorbed on recalcitrant Fe oxides
6	0.2 mol/L $[NH_4]_2C_2O_4$/0.17 mol/L $C_2H_2O_4$, 6 h, one repetition	Recalcitrant Fe oxides (magnetite)	As co-precipitated in recalcitrant Fe oxides
7	16 mol/L HNO_3, 2 h, one repetition	Fe(II) sulphides (mackinawite and pyrite)	As-bearing sulphides

3.2. Porewater depth profiles of major ions and trace elements

Fig. 4 shows that TDS in borehole S1 was higher near the water table with a minimum at 15 m depth, increasing towards the base of the aquifer. The same behaviour occurs for the less reactive dissolved species, such as Cl^-, Br^-, and SO_4^{2-}, often considered environmental tracers in oxidizing environments (Fetter, 2004). Conversely in S2, TDS was higher in the centre of the aquifer with a maximum at 20 m depth, decreasing towards the base of the aquifer. Cations such as Na^+ and Mg^{2+} mimic the conservative species in both S1 and S2, thus cation exchange reactions or carbonate dissolution/precipitation seem not to play a key role. K^+ in S2 shows an anomalous high peak, probably linked to areas affected by leakage from the sewerage system or to the presence of sewerage system overflow outlets that discharge water into the surface watercourse network, which subsequently reinfiltrate wastewaters in the unconfined aquifer. This was also highlighted by the Cl^- and Br^- molar ratio (approximately 1200) which was typical of urban wastewaters (Alcalá and Custodio, 2008) and by the presence of trace elements showing vertical trends similar to the major ions. In fact in S2, Zn, Si, and V concentration profiles were similar to Cl^- and K^+, thus probably coming from the same urban wastewater sources that are often enriched in these elements (Vittori Antisari et al., 2010).

NO_3^- tends to increase towards the base of the aquifer in S1, while is lower in S2 indicating complex groundwater pathways. In fact, NO_3^- concentration from rainfall recharge in the area should be around the average value and standard deviation of 4.7 ± 5.7 mg/L, as recorded in Lombardy urban areas precipitation (Stevenazzi et al., 2020). Thus, higher values could be considered symptoms of urban leakage, given the lack of agricultural activities in the upgradient area (ESA, 2019). In any case, NO_3^- concentrations did not exceed the regulatory value of 50 mg/L, while NO_2^- exceed it locally, most probably because of incomplete heterotrophic denitrification phenomena due to the lack of labile DOC (Castaldelli et al., 2019; Mastrocicco et al., 2019; Robertson and Schiff, 2008) allowing NO_3^- and NO_2^- to be transported downstream even for long distances. DOC also shows a slight positive peak in the centre of the aquifer, but the concentrations were very low (less than 0.5 mg/L) and in line with the DOC expected in an upland detrital aquifer (Appelo and Postma, 2005). Fe and Mn concentration profiles indicate that reduction processes developed in micro niches hosted within the low permeability lenses (Jakobsen, 2007) or more probably transported along the flowpath from upgradient leaking sewers (Christensen et al., 2000). Nevertheless, in both cores oxic or sub-oxic conditions were prevailing as defined by Christensen et al. (2000), given that both Fe and Mn never reached 0.2 mg/L and NO_3^- was always present in both cores.

Fig. 3. Stratigraphic logs of S1 and S2 cores with description and grain size distribution. The water table position is also shown (blue line and triangle).

Fig. 4 also shows the most significant trace elements for the S1 and S2 cores, where the absence of total As and very low concentrations of total Cr can be noted, in fact these trace elements can be mobilized only in reducing environments (Davis et al., 1994). Al and Zn were found at very low concentrations since their mobility at neutral pH is limited (Edmunds and Smedley, 1996), albeit Zn peak in S2 was probably imputable to sewers leakage as previously postulated.

3.3. Batch experiments results

Fig. 5 shows the dissolution kinetics of TDS and the most relevant physical parameters and chemical species in solution like TDS, alkalinity, Ca^{2+}, ORP, dissolved O_2, and pH. As can be seen from the graph, TDS was very low at the beginning and increased asymptotically towards the equilibrium between solids and liquid phases. Equilibrium was reached only in the last weeks of testing in all the batches.

To help visualizing the dissolution trends throughout the unconfined aquifer, a fit with exponential line is drawn in Fig. 5 with a green line; only dissolved species with a Pearson coefficient (R) greater than 0.60 and a *p*-value lower than 0.005 have been plotted along with their equations with statistical indicators. The exponential coefficient provides the bulk first order kinetic dissolution and desorption rate *k* (day^{-1}) from aquifer material. It can be noticed that the *k* value of TDS is very similar to the one of alkalinity, this implies that the kinetic dissolution of carbonates to the water mineralization over short periods is pivotal as found in other batch experiments with aquifer material (Bearup et al., 2012). On the contrary, the pH (apart some peaks), tended to vary much more rapidly and stabilized after 60 days. The pH changes were mainly due to the dissolution of carbonates, although the *k* value of Ca^{2+} was higher, implying a probable contribution also from the cation exchange capacity of the matrix. In any case, the *k* values were within one order of magnitude with literature values of dolomite and calcite in similar batch experiments (Descourvieres et al., 2010) and field modelling (Herold et al., 2011). The ORP increased during time indicating prevailing oxic conditions, while dissolved O_2 initially decrease from the deionized water concentration (5.0 mg/L) to stabilize at approximately 3.0 mg/L after 40 days without further changes. This is an indication that biological activity was very limited at the end of the batch experiments due to the lack of organic substrates (Christensen et al., 2000).

Fig. 6 shows the dissolution kinetics of major ions and trace elements present in solution in the batches. While Na^+ and SO_4^{2-} show lower *k* values implying that equilibrium conditions were reached faster than for Mg^{2+} and Ca^{2+}, Cl^- and K^+ were characterized by less homogeneous trends. In any case, no exceedances of any parameter or species in solution with respect to the WHO drinking water limits (WHO, 2022) were detected. From the graphs it can be noted that As concentrations never exceed 1.0 μg/L, and Fe and Pb remained at low concentrations. This was imputable to the oxic conditions, and the slightly alkaline pH maintained throughout the duration of the experiment; while to significantly mobilize trace elements reducing and acidic conditions are necessary (Bearup et al., 2012). Sr, a vicariant of Ca^{2+} and Mg^{2+} in carbonates, behaved similarly to the previously described alkalis. The dissolution of the sedimentary organic matter present in the aquifer

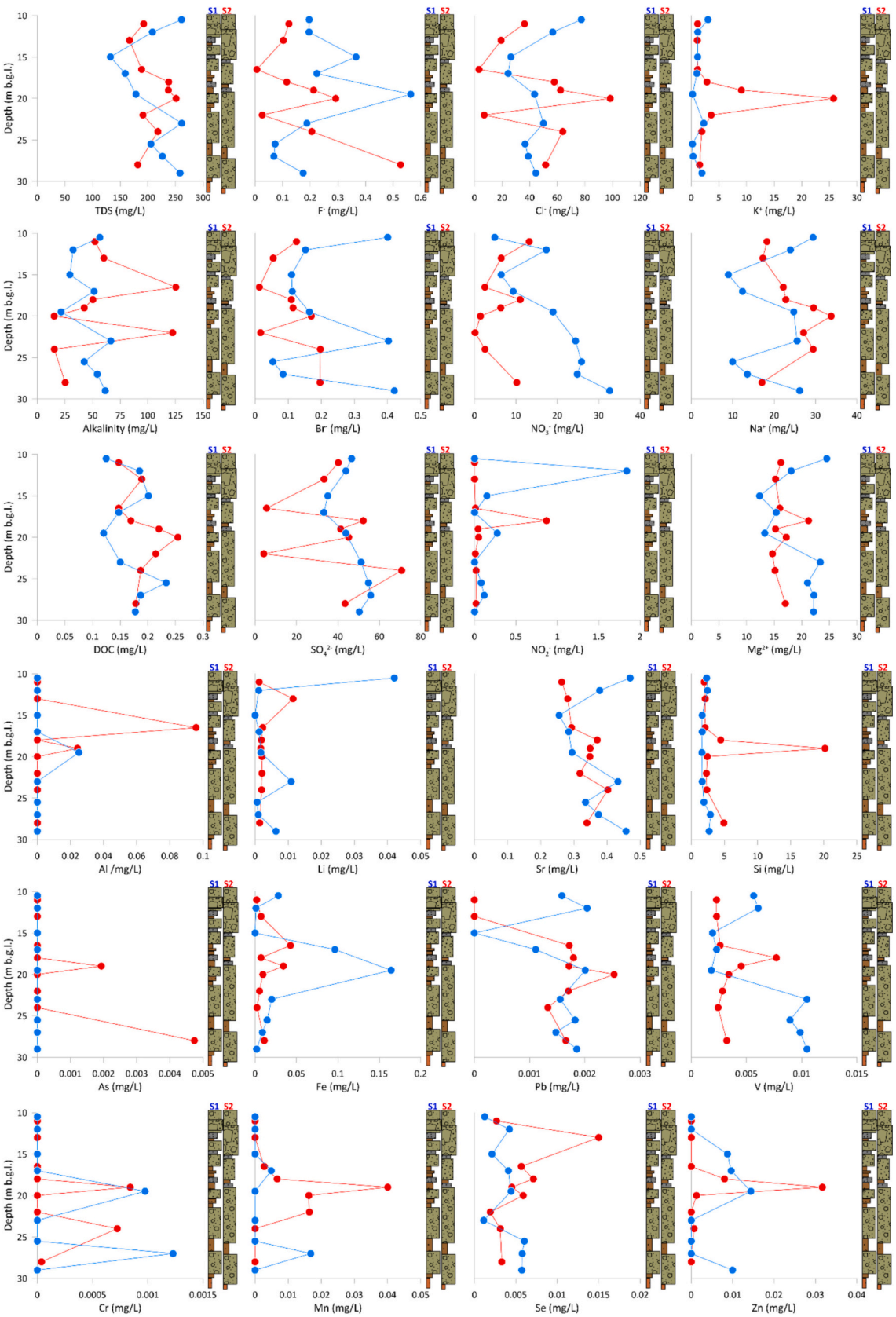

Fig. 4. Depth profiles of TDS, DOC and selected ions and trace elements for S1 (blue lines and dots) and for S2 (red lines and dots) cores. Their stratigraphic logs are also reported.

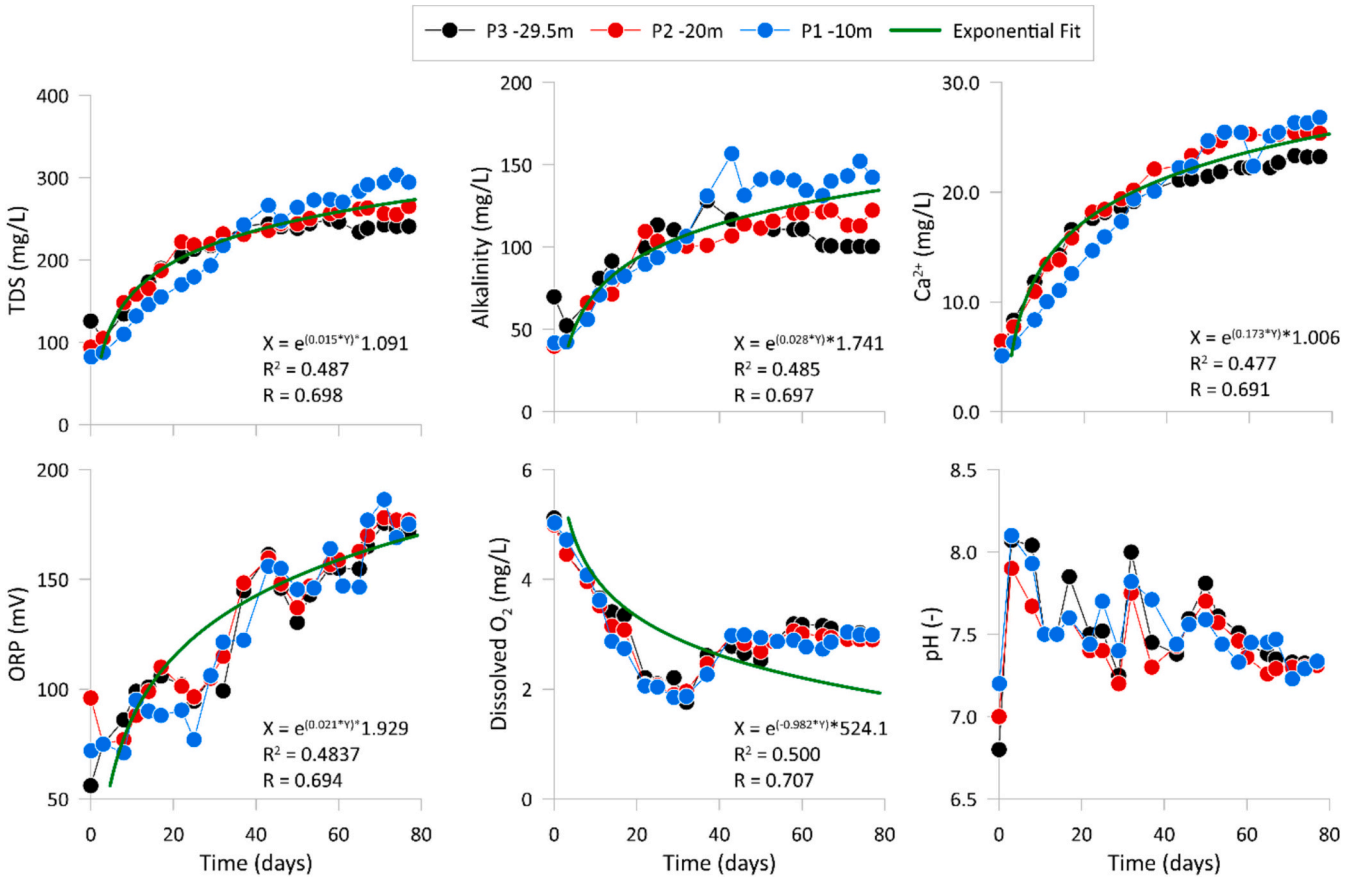

Fig. 5. Temporal trends of physical-chemical parameters, alkalinity and Ca^{2+} for the batch experiments with their exponential fit (green line).

matrix induced DOC to remain constant, albeit at very low concentrations. This confirmed that no electron donors were available to promote reducing conditions (Descourvieres et al., 2010). The organic N present in sedimentary organic matter was slightly mineralize firstly in NH_4^+, given the lack of NH_4^+ in the deionized water. The latter was in turn converted into NO_2^- and NO_3^- by nitrification. This is congruent with the disappearance of the initially available dissolved O_2, although this hypothesis should be confirmed by stable isotopes (Böhlke et al., 2006; Zhang et al., 2024). The other trace elements, being below detection limit, have not been graphed but the concentrations are reported in the Supplementary materials.

3.4. Sequential extraction results

From the graphs in Fig. 7, the distribution of As was homogeneous in the three sediment samples and in general characterized by very low concentrations in the first two extraction steps, in which As can usually be easily mobilized during MAR operations (Fakhreddine et al., 2021). In particular, the highest concentrations of As were found in step 5, the one that associates adsorbed As with recalcitrant Fe hydroxides, like magnetite (Sbarbati et al., 2020). Magnetite and siderite are found in the upstream rocks of the Early Triassic Servino formation, which is outcropping in Val Trompia along the Mella river course (De Donatis and Falletti, 1999). Locally the Servino formation hosts "strata-bound" mineralization rich in Mn-siderite and subordinate barite, with rare traces of Fe-sulphides with As inclusions (Martin et al., 2017). As was detected in solution only at very low concentrations (Fig. 6) and the prolonged exposure of the sediments to deionized water did not modify the As content in the different pools investigated by sequential extraction.

The pre- and post-batch experiments analyses did not statistically differ considering the experimental uncertainty of the measurements, represented by the error bars in Fig. 7. The only notable exception is Fe at step 4 in the upper part of the aquifer (S1-10m), where crystalline hydroxides, such as goethite and hematite, significantly increased after the batch experiments. This was possibly due to Fe leached by mineral phases (e.g., biotite) not targeted by the sequential extraction, that subsequently precipitated as hematite in oxic conditions. This finding highlights that mineral reactivity and secondary phases formation occurred even in these relatively short-term batch experiments, at least near the water table. If Fe-(oxyhydr)oxide recrystallization can occur during batch tests, the long-term stability of As bound to these phases under repeated MAR-induced redox/saturation cycles remains uncertain and still deserves more research.

In fact, even if the results of the sequential extraction showed that As was not remobilized by a single injection of deionized water, column experiments should be implemented in future studies to quantify As and other trace elements mobility with repeated cycles. In particular, the redox conditions in this shallow unconfined aquifer are not expected to change abruptly due to background oxic and sub-oxic conditions combined with limited DOC availability, but ionic strength and pH shifts induced by high purity water injection cycles should be better elucidated in future studies. Finally, the timescale of injections in full scale MAR via pumping wells for aquifer storage and recovery is often of months (Fakhreddine et al., 2021), thus the batch experiments here performed are representative only of a single cycle; but if the wells are operated in continuous injection mode, the attainment of hydrochemical equilibrium in batches could be considered representative of longer timescales.

4. Conclusions

The stratigraphic logs of S1 and S2 cores showed very permeable

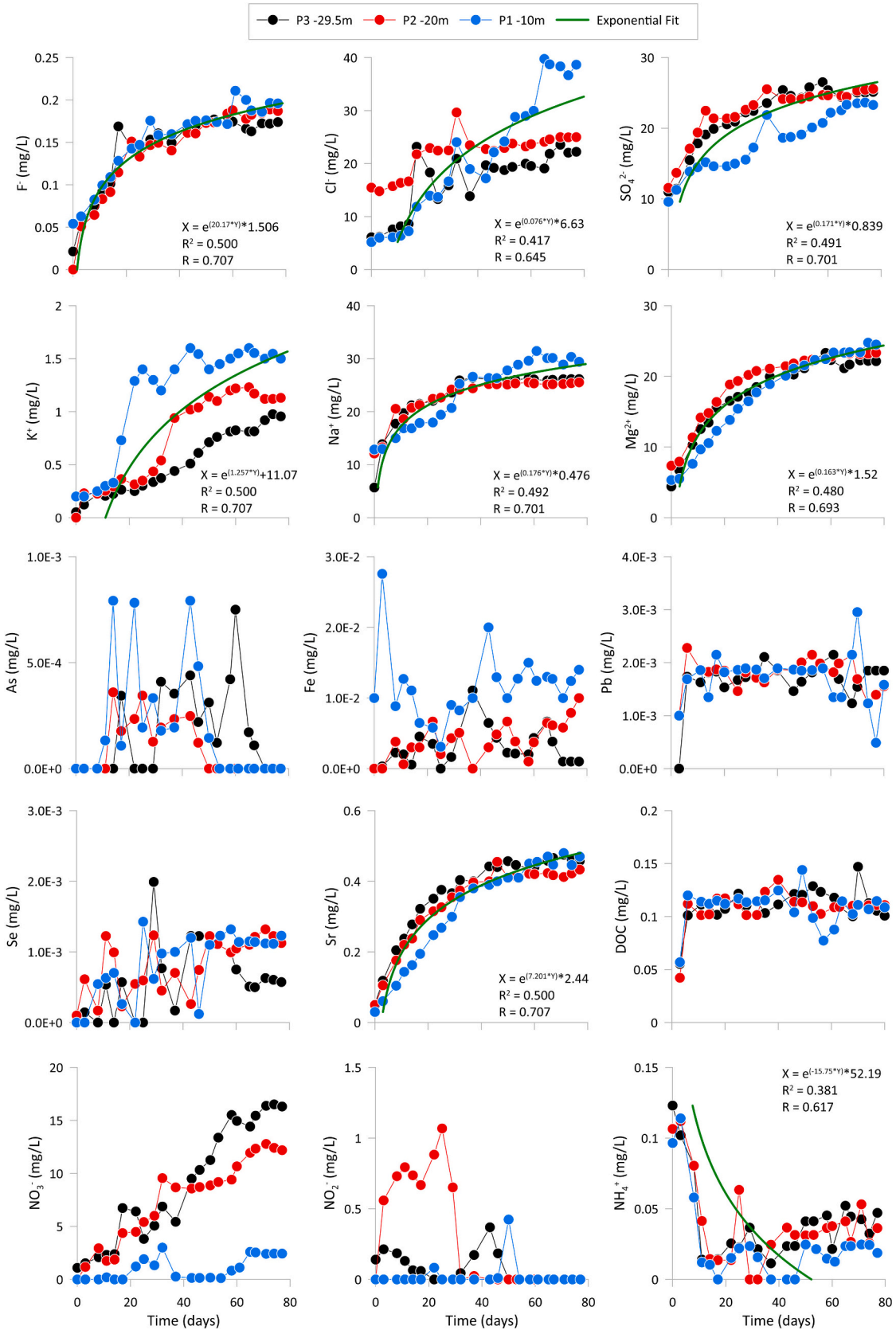

Fig. 6. Temporal trends of selected major ions, trace elements, and DOC for the batch experiments and their exponential fit (green line).

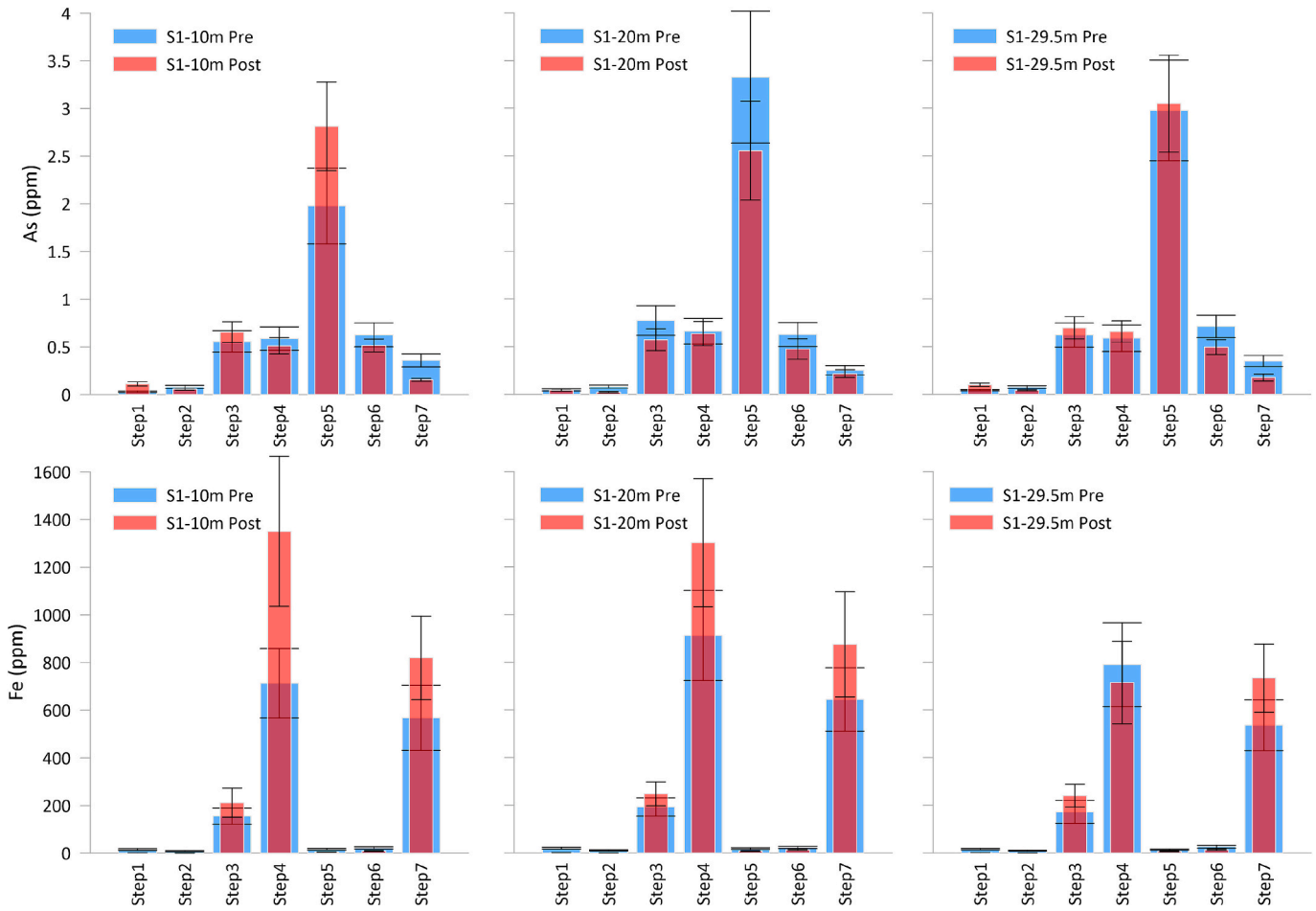

Fig. 7. Pre and post concentrations of As and Fe in the different target phases of the sequential extraction, for the three selected samples (S1-10, S1-20, and S1-29.5). The error bars represent the standard deviation of 3 replicas. Mean values of pre and post steps were not significantly different from each other (Tukey's HSD, $*P < 0.05$), except for the Fe Step4 of S1–10m.

gravel layers that will allow considerable volumes to be injected into the aquifer. The site, whose closeness to A2A facilities could favour logistics during design, construction, and operation phases, is therefore optimal for the possible water injection plant. Profile analyses by porewater extraction from S1 and S2 cores were pivotal in delineating the relevant redox processes and conditions within the target aquifer, as well as urban sources of pollution and their heterogeneities. Batch results demonstrated that MAR could help to decrease (via dilution by high purity waters) the potential inorganic contaminants coming from upgradient sources. Sequential extraction results for As showed that it was included in stable solid phases in oxidizing environments, therefore injections of high purity water is unlikely to mobilize this and other trace elements present at the site. Nevertheless, the finding that Fe-(oxyhydr) oxides recrystallized during the batch experiments highlighted the need of additional studies to proof the concept of As stability over repeated injection cycles.

This research is a first step, to be confirmed in the future with a small-scale injection of water to proof the concepts here drafted. The proposed characterization framework could be adopted in similar environments to estimate the potential release of heavy-metals(loid)s and biogeochemical reactions triggered by MAR, tailoring the design of pilot or full-scale implementation plants.

CRediT authorship contribution statement

Nicolò Colombani: Writing – original draft, Supervision, Software, Methodology, Conceptualization. **Abraham Ofori:** Writing – review & editing, Investigation, Formal analysis. **Jonathan Domizi:** Investigation, Formal analysis, Data curation. **Matteo Gisolo:** Writing – review & editing, Validation, Investigation. **Silene Itala Cresseri:** Writing – review & editing, Investigation. **Micòl Mastrocicco:** Writing – review & editing, Validation, Supervision, Resources, Project administration, Funding acquisition, Conceptualization.

Declaration of competing interest

The authors declare the following financial interests/personal relationships which may be considered as potential competing interests: Nicolo' Colombani reports financial support was provided by A2A CICLO IDRICO SPA. Abraham Ofori reports financial support was provided by A2A CICLO IDRICO SPA. Micol Mastrocicco reports financial support was provided by A2A CICLO IDRICO SPA. Joanathan Domizi reports financial support was provided by A2A CICLO IDRICO SPA. Matteo Gisolo reports a relationship with A2A CICLO IDRICO SPA that includes: employment. Silene Itala Cresseri reports a relationship with A2A CICLO IDRICO SPA that includes: employment.

Data availability

Data will be made available on request.

Acknowledgements

This research funded by a grant provided by "A2A Ciclo Idrico S.P.

A." to the non-profit organization "Consorzio Futuro in Ricerca".

Appendix A. Supplementary data

Supplementary data to this article can be found online at https://doi.org/10.1016/j.scitotenv.2025.180787.

References

Alcalá, F.J., Custodio, E., 2008. Using the Cl/Br ratio as a tracer to identify the origin of salinity in aquifers in Spain and Portugal. J. Hydrol. 359 (1–2), 189–207. https://doi.org/10.1016/j.jhydrol.2008.06.028.

Appelo, C.A.J., Postma, D., 2005. Geochemistry, Groundwater and Pollution. CRC press, London, UK, p. 683. https://doi.org/10.1201/9781439833544.

Balestrini, R., Delconte, C.A., Sacchi, E., Buffagni, A., 2021. Groundwater-dependent ecosystems as transfer vectors of nitrogen from the aquifer to surface waters in agricultural basins: the fontanili of the Po Plain (Italy). Sci. Total Environ. 753, 141995. https://doi.org/10.1016/j.scitotenv.2020.141995.

Bearup, L.A., Navarre-Sitchler, A.K., Maxwell, R.M., McCray, J.E., 2012. Kinetic metal release from competing processes in aquifers. Environ. Sci. Technol. 46 (12), 6539–6547. https://doi.org/10.1021/es203586y.

Böhlke, J.K., Smith, R.L., Miller, D.N., 2006. Ammonium transport and reaction in contaminated groundwater: application of isotope tracers and isotope fractionation studies. Water Resour. Res. 42 (5), W05411. https://doi.org/10.1029/2005WR004349.

Bonomi, T., Fumagalli, L., Rotiroti, M., Bellani, A., Cavallin, A., 2014. The hydrogeological well database TANGRAM©: a tool for data processing to support groundwater assessment. Acque Sotterranee Ital. J. Groundwater 3 (2). https://doi.org/10.7343/as-072-14-0098.

Braca, G., Bussettini, M., Gafà, R.M., Monti, G.M., Martarelli, L., Silvi, A., La Vigna, F., 2022. The nationwide water budget estimation in the light of the new permeability map of Italy. Acque Sotterranee Ital. J. Groundwater 11 (3), 31–39. https://doi.org/10.7343/as-2022-575.

Brescia Municipality Environmental Report, 2022. Valutazione Ambientale Strategica. Available at: https://www.comune.brescia.it/lfs/servizi/urbanistica/PGT/Documents/QUARTA%20VARIANTE_2022/Allegato%20n_1_quadro%20conoscitivo_Rapp.Ambientale.pdf.

Castaldelli, G., Colombani, N., Soana, E., Vincenzi, F., Fano, E.A., Mastrocicco, M., 2019. Reactive nitrogen losses via denitrification assessed in saturated agricultural soils. Geoderma 337, 91–98. https://doi.org/10.1016/j.geoderma.2018.09.018.

Castaldini, D., Marchetti, M., Norini, G., Vandelli, V., Zuluaga Vélez, M.C., 2019. Geomorphology of the central Po plain, Northern Italy. J. Maps 15 (2), 780–787. https://doi.org/10.1080/17445647.2019.1673222.

Christensen, T.H., Bjerg, P.L., Banwart, S.A., Jakobsen, R., Heron, G., Albrechtsen, H.J., 2000. Characterization of redox conditions in groundwater contaminant plumes. J. Contam. Hydrol. 45 (3–4), 165–241. https://doi.org/10.1016/S0169-7722(00)00109-1.

Colombani, N., Mastrocicco, M., Prommer, H., Sbarbati, C., Petitta, M., 2015. Fate of arsenic, phosphate and ammonium plumes in a coastal aquifer affected by saltwater intrusion. J. Contam. Hydrol. 179, 116–131. https://doi.org/10.1016/j.jconhyd.2015.06.003.

Cook, S., Peacock, M., Evans, C.D., Page, S.E., Whelan, M.J., Gauci, V., Kho, L.K., 2017. Quantifying tropical peatland dissolved organic carbon (DOC) using UV-visible spectroscopy. Water Res. 155, 229–235. https://doi.org/10.1016/j.watres.2017.02.059.

Davis, A., Kempton, J.H., Nicholson, A., Yare, B., 1994. Groundwater transport of arsenic and chromium at a historical tannery, Woburn, Massachusetts, USA. Appl. Geochem. 9 (5), 569–582. https://doi.org/10.1016/0883-2927(94)90019-1.

De Donatis, S., Falletti, P., 1999. The Early Triassic Servino Formation of the Monte Guglielmo area and relationships with the Servino of Trompia and Camonica Valleys (Brescian Prealps, Lombardy). Mem. Sci. Geol. 51 (1), 91–101.

Descourvieres, C., Prommer, H., Oldham, C., Greskowiak, J., Hartog, N., 2010. Kinetic reaction modeling framework for identifying and quantifying reductant reactivity in heterogeneous aquifer sediments. Environ. Sci. Technol. 44 (17), 6698–6705. https://doi.org/10.1021/es101661u.

Dillon, P., Stuyfzand, P., Grischek, T., Lluria, M., Pyne, R.D.G., Jain, R.C., Sapiano, M., 2019. Sixty years of global progress in managed aquifer recharge. Hydrogeol. J. 27 (1), 1–30. https://doi.org/10.1007/s10040-018-1841-z.

Edmunds, W.M., Smedley, P.L., 1996. Groundwater geochemistry and health: an overview. Geol. Soc. Lond. Spec. Publ. 113 (1), 91–105. https://doi.org/10.1144/GSL.SP.1996.113.01.08.

ESA, European Environment Agency, 2019. CORINE Land Cover 2018 (raster 100m), Europe, 2017–2018. Available at:, Copernicus Land Monitoring Service. https://land.copernicus.eu/pan-european/corine-land-cover/clc2018.

Fakhreddine, S., Dittmar, J., Phipps, D., Dadakis, J., Fendorf, S., 2015. Geochemical triggers of arsenic mobilization during managed aquifer recharge. Environ. Sci. Technol. 49 (13), 7802–7809. https://doi.org/10.1021/acs.est.5b01140.

Fakhreddine, S., Prommer, H., Gorelick, S.M., Dadakis, J., Fendorf, S., 2020. Controlling arsenic mobilization during managed aquifer recharge: the role of sediment heterogeneity. Environ. Sci. Technol. 54 (14), 8728–8738. https://doi.org/10.1021/acs.est.0c00794.

Fakhreddine, S., Prommer, H., Scanlon, B.R., Ying, S.C., Nicot, J.P., 2021. Mobilization of arsenic and other naturally occurring contaminants during managed aquifer recharge: a critical review. Environ. Sci. Technol. 55 (4), 2208–2223. https://doi.org/10.1021/acs.est.0c07492.

Fetter, C.W., 2004. Applied Hydrogeology, fourth ed. Macmillan, New York USA.

Giuliano, G., 1995. Ground water in the Po basin: some problems relating to its use and protection. Sci. Total Environ. 171 (1–3), 17–27. https://doi.org/10.1016/0048-9697(95)04682-1.

Guo, Z., Chen, K., Yi, S., Zheng, C., 2023. Response of groundwater quality to river-aquifer interactions during managed aquifer recharge: a reactive transport modeling analysis. J. Hydrol. 616, 128847. https://doi.org/10.1016/j.jhydrol.2022.128847.

Herold, M., Greskowiak, J., Ptak, T., Prommer, H., 2011. Modelling of an enhanced PAH attenuation experiment and associated biogeochemical changes at a former gasworks site in southern Germany. J. Contam. Hydrol. 119 (1–4), 99–112. https://doi.org/10.1016/j.jconhyd.2010.09.012.

ISPRA, 2024. National boreholes database. Available at: https://sgi2.isprambiente.it/viewersgi2/.

Jakobsen, R., 2007. Redox microniches in groundwater: a model study on the geometric and kinetic conditions required for concomitant Fe oxide reduction, sulfate reduction, and methanogenesis. Water Resour. Res. 43, W12S12. https://doi.org/10.1029/2006WR005663.

Keon, N.E., Swartz, C.H., Brabander, D.J., Harvey, C., Hemond, H.F., 2001. Validation of an arsenic sequential extraction method for evaluating mobility in sediments. Environ. Sci. Technol. 35, 2778–2784. https://doi.org/10.1021/es001511o.

Lasagna, M., De Luca, D.A., Franchino, E., 2016. Nitrate contamination of groundwater in the western Po Plain (Italy): the effects of groundwater and surface water interactions. Environ. Earth Sci. 75, 1–16. https://doi.org/10.1007/s12665-015-5039-6.

Levintal, E., Kniffin, M.L., Ganot, Y., Marwaha, N., Murphy, N.P., Dahlke, H.E., 2022. Agricultural managed aquifer recharge (Ag-MAR)—a method for sustainable groundwater management: a review. Crit. Rev. Environ. Sci. Technol. 53 (3), 291–314. https://doi.org/10.1080/10643389.2022.2050160.

Levintal, E., Huang, L., García, C.P., Coyotl, A., Fidelibus, M.W., Horwath, W.R., Mazza Rodrigues, J.L., Dahlke, H.E., 2023. Nitrogen fate during agricultural managed aquifer recharge: linking plant response, hydrologic, and geochemical processes. Sci. Total Environ. 864, 161206. https://doi.org/10.1016/j.scitotenv.2022.16120.

Maeng, S.K., Sharma, S.K., Abel, C.D., Magic-Knezev, A., Amy, G.L., 2011. Role of biodegradation in the removal of pharmaceutically active compounds with different bulk organic matter characteristics through managed aquifer recharge: batch and column studies. Water Res. 45 (16), 4722–4736. https://doi.org/10.1016/j.watres.2011.05.043.

Marchetti, M., Bondesan, M., Castaldini, D., Cremaschi, M., Gasperi, G., Motta, M., Tellini, C., Trombino, L., 2001. Forme e depositi fluviali, fluvioglaciali, lacustri-fluvial, fluvioglacial and lacustrine forms and deposits. Suppl. Geogr. Fis. Dinam. Quat. 73–104.

Martin, S., Toffolo, L., Moroni, M., Montorfano, C., Secco, L., Agnini, C., Nimis, P., Tumiati, S., 2017. Siderite deposits in northern Italy: Early Permian to Early Triassic hydrothermalism in the Southern Alps. Lithos 284, 276–295. https://doi.org/10.1016/j.lithos.2017.04.002.

Martinelli, G., Dadomo, A., De Luca, D.A., Mazzola, M., Lasagna, M., Pennisi, M., Pilla, G., Sacchi, E., Saccon, P., 2018. Nitrate sources, accumulation and reduction in groundwater from Northern Italy: insights provided by a nitrate and boron isotopic database. Appl. Geochem. 91, 23–35. https://doi.org/10.1016/j.apgeochem.2018.01.011.

Martinez, M.B., Widdowson, M.A., Bott, C., Holloway, D., Heisig-Mitchell, J., Wilson, C., 2022. Demonstration of managed aquifer recharge in a coastal plain aquifer: lessons learned. Groundwater 60 (5), 668–674. https://doi.org/10.1111/gwat.13197.

Mastrocicco, M., Colombani, N., Castaldelli, G., 2019. Direct measurement of dissolved dinitrogen to refine reactive modelling of denitrification in agricultural soils. Sci. Total Environ. 647, 134–140. https://doi.org/10.1016/j.scitotenv.2018.07.428.

Miller, W.P., Miller, D.M., 1987. A micro-pipette method for soil mechanical analysis. Commun. Soil Sci. Plant Anal. 18 (1), 1–15. https://doi.org/10.1080/00103628709367799.

Montanari, A., 2012. Hydrology of the Po River: looking for changing patterns in river discharge. Hydrol. Earth Syst. Sci. 16, 3739–3747. https://doi.org/10.5194/hess-16-3739-2012.

Mumberg, T., Ahrens, L., Wanner, P., 2024. Managed aquifer recharge as a potential pathway of contaminants of emerging concern into groundwater systems–a systematic review. Chemosphere, 143030. https://doi.org/10.1016/j.chemosphere.2024.143030.

Musolino, D., Vezzani, C., Massarutto, A., 2018. Drought management in the Po river basin, Italy. In: Drought: Sci. Policy, pp. 201–215. https://doi.org/10.1002/9781119017073.ch11.

Ori, G.G., 1993. Continental depositional systems of the Quaternary of the Po Plain (northern Italy). Sediment. Geol. 83 (1–2), 1–14. https://doi.org/10.1016/S0037-0738(10)80001-6.

Pena, M.E., Korfiatis, G.P., Patel, M., Lippincott, L., Meng, X., 2005. Adsorption of As(V) and As(III) by nanocrystalline titanium dioxide. Water Res. 39 (11), 2327–2337. https://doi.org/10.1016/j.watres.2005.04.006.

Pili, N., Alberico, E., Confalonieri, M., Pastore, M., Bortoletto, R., Molinari, A., 2017. SIN Brescia – Caffaro: risultati monitoraggio acque sotterranee. Indagine geochimica e piezometrica, Gennaio 2015. Geol. Tec. Ambient. 17, 35–46.

Pinardi, M., Soana, E., Severini, E., Racchetti, E., Celico, F., Bartoli, M., 2022. Agricultural practices regulate the seasonality of groundwater-river nitrogen exchanges. Agric. Water Manag. 273, 107904. https://doi.org/10.1016/j.agwat.2022.107904.

Pokhrel, P., Zhou, Y., Smits, F., Kamps, P., Olsthoorn, T., 2023. Numerical simulation of a managed aquifer recharge system designed to supply drinking water to the city of

Amsterdam, The Netherlands. Hydrogeol. J. 31 (5), 1291–1309. https://doi.org/10.1007/s10040-023-02659-w.
Racz, A.J., Fisher, A.T., Schmidt, C.M., Lockwood, B.S., Huertos, M.L., 2012. Spatial and temporal infiltration dynamics during managed aquifer recharge. Groundwater 50 (4), 562–570. https://doi.org/10.1111/j.1745-6584.2011.00875.x.
Regnery, J., Wing, A.D., Kautz, J., Drewes, J.E., 2016. Introducing sequential managed aquifer recharge technology (SMART)–from laboratory to full-scale application. Chemosphere 154, 8–16. https://doi.org/10.1016/j.chemosphere.2016.03.097.
Riedel, T., Kübeck, C., Quirin, M., 2022. Legacy nitrate and trace metal (Mn, Ni, As, Cd, U) pollution in anaerobic groundwater: quantifying potential health risk from "the other nitrate problem". Appl. Geochem. 139, 105254. https://doi.org/10.1016/j.apgeochem.2022.105254.
Robertson, W.D., Schiff, S.L., 2008. Persistent elevated nitrate in a riparian zone aquifer. J. Environ. Qual. 37 (2), 669–679. https://doi.org/10.2134/jeq2007.0102.
Ronen-Eliraz, G., Russak, A., Nitzan, I., Guttman, J., Kurtzman, D., 2017. Investigating geochemical aspects of managed aquifer recharge by column experiments with alternating desalinated water and groundwater. Sci. Total Environ. 574, 1174–1181. https://doi.org/10.1016/j.scitotenv.2016.09.075.
Rotiroti, M., Sacchi, E., Caschetto, M., Zanotti, C., Fumagalli, L., Biasibetti, M., Bonomi, T., Leoni, B., 2023. Groundwater and surface water nitrate pollution in an intensively irrigated system: sources, dynamics and adaptation to climate change. J. Hydrol. 623, 129868. https://doi.org/10.1016/j.jhydrol.2023.129868.
Sacchi, E., Acutis, M., Bartoli, M., Brenna, S., Delconte, C.A., Laini, A., Pennisi, M., 2013. Origin and fate of nitrates in groundwater from the central Po plain: insights from isotopic investigations. Appl. Geochem. 34, 164–180. https://doi.org/10.1016/j.apgeochem.2013.03.00.
Sadiq, M., 1990. Arsenic chemistry in marine environments – a comparison between theoretical and field observations. Mar. Chem. 31, 285–297. https://doi.org/10.1016/0304-4203(90)90043-C.
Sbarbati, C., Barbieri, M., Barron, A., Bostick, B., Colombani, N., Mastrocicco, M., Prommer, H., Passaretti, S., Zheng, Y., Petitta, M., 2020. Redox dependent arsenic occurrence and partitioning in an industrial coastal aquifer: evidence from high spatial resolution characterization of groundwater and sediments. Water 12 (10), 2932. https://doi.org/10.3390/w12102932.
Schafer, D., Sun, J., Jamieson, J., Siade, A., Atteia, O., Seibert, S., Higginson, S., Prommer, H., 2021. Fluoride release from carbonate-rich fluorapatite during managed aquifer recharge: model-based development of mitigation strategies. Water Res. 193, 116880. https://doi.org/10.1016/j.watres.2021.116880.
Schiavo, M., Giambastiani, B.M.S., Greggio, N., Colombani, N., Mastrocicco, M., 2024. Geostatistical assessment of groundwater arsenic contamination in the Padana Plain. Sci. Total Environ. 931, 172998. https://doi.org/10.1016/j.scitotenv.2024.172998.
Stevenazzi, S., Camera, C.A.S., Masetti, M., Azzoni, R.S., Ferrari, E.S., Tiepolo, M., 2020. Atmospheric nitrogen depositions in a highly human-impacted area. Water Air Soil Pollut. 231, 276. https://doi.org/10.1007/s11270-020-04613-y.
Suda, A., Makino, T., 2016. Functional effects of manganese and iron oxides on the dynamics of trace elements in soils with a special focus on arsenic and cadmium: a review. Geoderma 270, 68–75. https://doi.org/10.1016/j.geoderma.2015.12.01.
Sun, J., Chillrud, S.N., Mailloux, B.J., Bostick, B.C., 2016. In situ magnetite formation and longterm arsenic immobilization under advective flow conditions. Environ. Sci. Technol. 50, 10162–10171. https://doi.org/10.1021/acs.est.6b02362.
Tiwari, A.K., De Maio, M., Amanzio, G., 2017. Evaluation of metal contamination in the groundwater of the Aosta Valley Region, Italy. Int. J. Environ. Res. 11 (3), 291–300. https://doi.org/10.1007/s41742-017-0027-1.
Vergara-Sáez, C., Prommer, H., Siade, A.J., Sun, J., Higginson, S., 2024. Process-based and probabilistic quantification of Co and Ni mobilization risks induced by managed aquifer recharge. Environ. Sci. Technol. 58 (17), 7567–7576. https://doi.org/10.1021/acs.est.3c10583.
Vittori Antisari, L., Trivisano, C., Gessa, C., Gherardi, M., Simoni, A., Vianello, G., Zamboni, N., 2010. Quality of municipal wastewater compared to surface waters of the river and artificial canal network in different areas of the eastern Po valley (Italy). Water Qual Expo Health 2 (1), 1–13. https://doi.org/10.1007/s12403-009-0020-9.
Wang, F., van Halem, D., Ding, L., Bai, Y., Lekkerkerker-Teunissen, K., van der Hoek, J. P., 2018. Effective removal of bromate in nitrate-reducing anoxic zones during managed aquifer recharge for drinking water treatment: laboratory-scale simulations. Water Res. 130, 88–97. https://doi.org/10.1016/j.watres.2017.11.052.
WHO (World Health Organization), 2022. Guidelines for Drinking-Water Quality: Fourth Edition Incorporating the First Addendum. World Health Organization, Geneva. Available at: https://www.who.int/publications/i/item/9789240045064.
Wu, P., Shu, L., Comte, J.C., Zuo, Q., Wang, M., Li, F., Chen, H., 2021. The effect of typical geological heterogeneities on the performance of managed aquifer recharge: physical experiments and numerical simulations. Hydrogeol. J. 29 (6), 2107–2125. https://doi.org/10.1007/s10040-019-02033-9.
Zanchi, M., Zapperi, S., Zanotti, C., Rotiroti, M., Bonomi, T., Gomarasca, S., Bocchi, S., La Porta, C.A., 2022. A pipeline for monitoring water pollution: the example of heavy metals in Lombardy waters. Heliyon 8 (12), e12435. https://doi.org/10.1016/j.heliyon.2022.e12435.
Zanotti, C., Rotiroti, M., Caschetto, M., Redaelli, A., Bozza, S., Biasibetti, M., Mostarda, L., Fumagalli, L., Bonomi, T., 2022. A cost-effective method for assessing groundwater well vulnerability to anthropogenic and natural pollution in the framework of water safety plans. J. Hydrol. 613, 128473. https://doi.org/10.1016/j.jhydrol.2022.128473.
Zanotti, C., Rotiroti, M., Redaelli, A., Caschetto, M., Fumagalli, L., Stano, C., Sartirana, D., Bonomi, T., 2023. Multivariate time series clustering of groundwater quality data to develop data-driven monitoring strategies in a historically contaminated urban area. Water 15 (1), 148. https://doi.org/10.3390/w15010148.
Zhang, Z., Furman, A., 2021. Soil redox dynamics under dynamic hydrologic regimes-A review. Science of the Total Environment 763, 143026. https://doi.org/10.1016/j.scitotenv.2020.143026.
Zhang, L., Zhang, Z., Huang, X., Zhang, J., Schneidewind, U., Krause, S., Jin, M., Xing, L., Zhan, H., 2024. Ammonium enrichment, nitrate attenuation and nitrous oxide production along groundwater flow paths: carbon isotopic and DOM optical evidence. J. Hydrol. 632, 130943. https://doi.org/10.1016/j.jhydrol.2024.13094.
Zhou, T., Ruud, N., Šimůnek, J., Brunetti, G., Levintal, E., García, C.P., Dahlke, H.E., 2024. The impact of managed aquifer recharge on the fate and transport of pesticides in agricultural soils. Water Res. 267, 122442. https://doi.org/10.1016/j.watres.2024.122442.